

Article

Selecting Surface Inclination for Maximum Solar Power

Ioannis-Panagiotis Raptis ^{1,2,*} , Anna Moustaka ³, Panagiotis Kosmopoulos ^{1,*}  and Stelios Kazadzis ⁴ 

- ¹ Institute for Environmental Research and Sustainable Development, National Observatory of Athens, 15236 Athens, Greece
- ² Department of Geology and Geoenvironment, National and Kapodistrian University of Athens, 15784 Athens, Greece
- ³ Institute for Astronomy, Astrophysics, Space Applications and Remote Sensing, National Observatory of Athens, 15236 Athens, Greece; annamstk@noa.gr
- ⁴ Physicalisch-Meteorologisches Observatorium Davos—World Radiation Center, 7260 Davos, Switzerland; stelios.kazadzis@pmodwrc.ch
- * Correspondence: piraptis@noa.gr (I.-P.R.); pkosmo@noa.gr (P.K.)

Abstract: Maximum efficiency of surfaces that exploit solar energy, including Photovoltaic Panels and Thermal collectors, is achieved by installing them in a certain inclination (tilt). Most common approach is to select an inclination angle equal to the location's latitude. This is based on the astronomical calculations of the sun's position throughout the year but ignores meteorological factors. Cloud coverage and aerosols tend to change the direct irradiance but also the radiance sky distribution, thus horizontal surfaces receive larger amounts than tilted ones in specific atmospheric conditions (e.g., cases of cloud presence). In the present study we used 15 years of data, from 25 cities in Europe and North Africa in order to estimate the optimal tilt angle and the related energy benefits based in real atmospheric conditions. Data were retrieved from Copernicus Atmospheric Monitoring Service (CAMS). Four diffuse irradiance, various models are compared, and their differences are evaluated. Equations, extracted from solar irradiance and cloud properties regressions, are suggested to estimate the optimal tilt angle in regions, where no climatological data are available. In addition, the impact of cloud coverage is parameterized using the Cloud Modification Factor (CMF) and an equation is proposed to estimate the optimal tilt angle. A realistic representation of the photovoltaic energy production and a subsequent financial analysis were additionally performed. The results are able to support the prognosis of energy outcome and should be part of energy planning and the decision making for optimum solar power exploitation into the international clean energy transitions. Finally, results are compared to a global study and differences on the optimal tilt angle at cities of Northern Europe is presented.

Keywords: solar energy; tilt angle; Europe; North Africa; clouds; aerosols; inclination



Citation: Raptis, I.-P.; Moustaka, A.; Kosmopoulos, P.; Kazadzis, S. Selecting Surface Inclination for Maximum Solar Power. *Energies* **2022**, *15*, 4784. <https://doi.org/10.3390/en15134784>

Academic Editor: Alban Kuriqi

Received: 31 May 2022

Accepted: 28 June 2022

Published: 29 June 2022

Publisher's Note: MDPI stays neutral with regard to jurisdictional claims in published maps and institutional affiliations.



Copyright: © 2022 by the authors. Licensee MDPI, Basel, Switzerland. This article is an open access article distributed under the terms and conditions of the Creative Commons Attribution (CC BY) license (<https://creativecommons.org/licenses/by/4.0/>).

1. Introduction

Energy needs of societies are steadily increasing, while an urgent need of transition from fossil fuels to renewable energy sources is ascertained in studies and reports [1–3]. Solar energy is one of the most safe and sustainable energy sources and its use is expected to rise significantly over the next decades [4,5]. Most widely applied approach for capturing solar energy is the installation of Photovoltaic (PV) surfaces on rooftops or in PV power plants. In order to maximize the outcome of PV systems, the surfaces usually are set at certain inclinations. The most effective approach is to install a solar tracking system, that will follow the sun during the day, but this is more expensive and also consumes energy to rotate [6]. Simpler installations are set at a constant inclination. Prognosis of the solar irradiance incident on the inclined surface is crucial for evaluating the electric output and maximizing the efficiency of the system. Basic astronomic calculations provide an estimation for the tilt angle of the installation, assuming clear sky conditions (e.g., [7]).

The simulation of the sun path at a specific location, during all days of year, leads to the preferred fixed angle of β equal with φ facing the equinox, where β is the optimal angle and φ the location's latitude [8]. In real conditions, the optimum angle is different due to atmospheric processes, caused basically by clouds and secondary by other particles such as aerosols. These facts lead to different approaches when designing PV set ups, depending on energy needs, available budget and climatological data. In case of cloud covered skies, for solar tracking PVs, the energy spent for rotating the system could overpass the captured from the panel and in this case a horizontal surface would be more beneficial. Additionally, other applications, such as solar thermal collectors [9] or greenhouses covers [10], need to select the tilt angle of surfaces aiming to receive maximum solar irradiance all year round. Azimuthal orientation is always preferably southwise at the North Hemisphere and northwise at the South Hemisphere [6].

Recent studies have been published, estimating the optimum tilt angle for maximum solar energy yield, at specific geographical regions [8,11–19]. In addition, the question of a global tool to calculate the ideal installation setup had been studied with the use of neural networks [20], other meteorological variables [21], Genetic Algorithms [22] and Particle-Swarm Optimization techniques [23]. Jacobson and Jadhav [24] have utilized PVWatts [25] database and Chinchilla [26], two databases (EnergyPlus and Baseline Surface Radiation Network—BSRN) in order to propose a global approach on calculating the optimum tilt angle, which in each case provided better results at different geographical areas. All the above-mentioned studies conclude optimal tilt angles, smaller than the latitude but the exact values for same regions differ mainly due to different training periods/data sets and assumptions made.

The main aspect of the present work is to assess the possibility of simple and uniform equations to calculate the most effective tilt angle at a location, considering cloud climatology at the given area. This prognosis is based on the past climatology, but it will be very close to the actual conditions for the coming decades, if there are no large deviations on cloud coverage. Additionally, an approach that uses the latitude as a proxy for these parameters (which is only valid in the studied area) have been developed. In order to achieve these semiempirical approaches, we have used hourly irradiance data for 25 cities for a 15-year period by CAMS as input to a diffuse irradiance model in order to calculate the incident irradiance at different tilt angles. This historic database then is exploited in order to estimate the optimal tilt angle at each city and aggregate the results in respect to latitude and clouds. Finally, a financial analysis of the benefits is presented. Our aim is to keep the suggested approaches as simple as possible, in order to be conveniently applied by users and to give prominence of exploiting publicly available databases such as CAMS for similar applications.

2. Data and Methods

2.1. Data Sets

Hourly data for the years 2005–2019 for 25 cities in Europe and North Africa (as shown in Figure 1), were used. This service can provide global (*GHI*), beam (*BHI*), diffuse (*DHI*) irradiance on horizontal plane at ground level for cloudless and real sky conditions and the irradiation on horizontal plane at the top of the atmosphere. These datasets are created by combining satellite images and model calculations for cloudless conditions, following the Heliosat-4 method [27].

The following quality control criteria were applied to hourly values and those outside the limits were rejected [28]:

- (i) $GHI \geq 0.19 \text{ W/m}^2$;
- (ii) $GHI \leq 1.12 \times I_{sc}$;
- (iii) $DHI \leq 1.1 \times GHI$;
- (iv) $DHI \leq 0.8 \times I_{sc}$, and
- (v) $BHI \leq I_{sc}$

where I_{sc} is the solar constant equal to 1366.1 W/m^2 [29]. Solar geometry parameters, such as azimuth angle (Az), zenith angle (Sza) and elevation (El) were estimated for all locations using astronomical calculations.

For parameterizing cloud influence we have used the variable Cloud Modification Factor (CMF) which is defined as the ratio of the actual GHI to the expected one in cloudless sky conditions [30]. Thus, changes in irradiance parametrized by the CMF represent the effect of clouds. To calculate this variable, we have used CMF ranges by definition from 0 (total darkness) to 1 (cloudless sky). CMF was calculated from the hourly ratio GHI divided by Clear sky GHI , in order to consider the influence of clouds to the results. Additionally, Aerosol Optical Depth (AOD at 550 nm dataset was retrieved from the same service. It should be highlighted that the CAMS product that is label as “clear sky”, includes AOD in the calculation, following the approach described in [31]. Hence, it should be described as cloud free, and the calculations presented here represent the combined effect of clouds and aerosols, while CMF describes only the cloud effect.

The selection of 25 cities across Europe and North Africa, 19 of them are capitals, maintaining a wide spatial distribution. In Africa, we have also selected 2 cities on the south of Sahara Desert, Aswan and Tamanrasset. The latter is below the tropic of cancer, which ends up a to a very different pattern of seasons and solar related variables. Although the subtropical areas, should be studied separately in the future, we decided to include Tamanrasset in this study, because of the high aerosol load and to have an outlier region to test the validity of the outcomes.

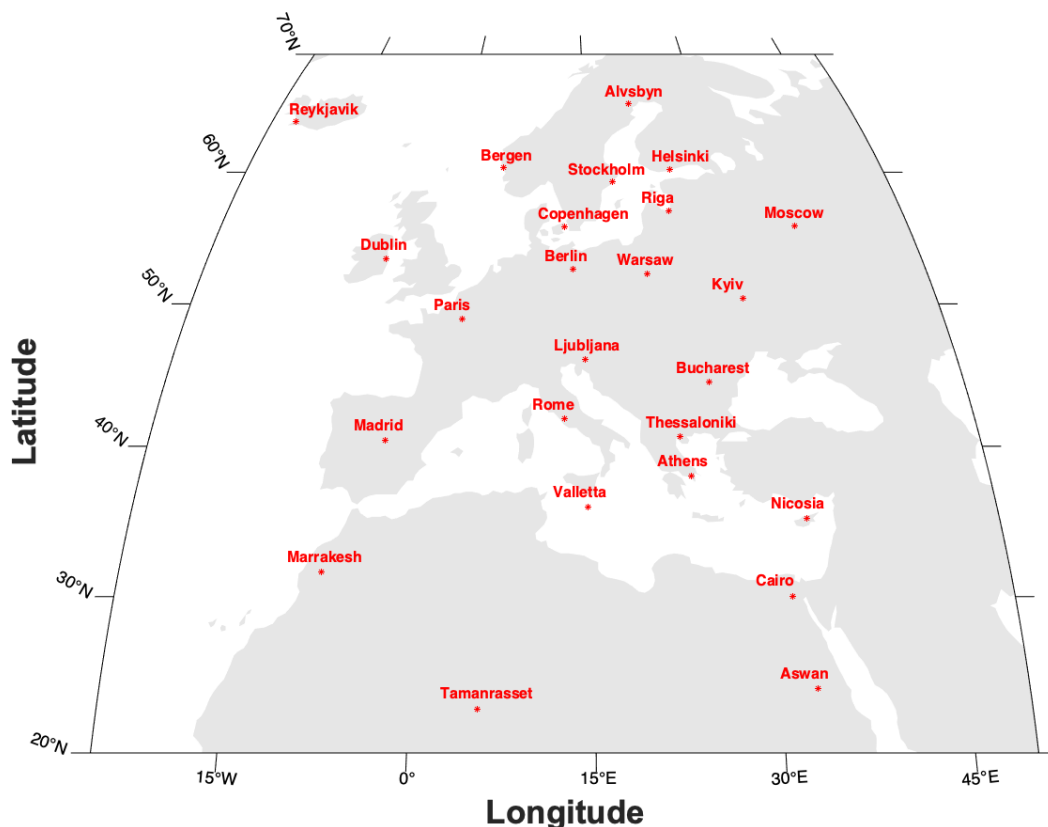


Figure 1. Locations of the Cities in Europe and North Africa selected for the study.

2.2. Diffuse Irradiance Models

A surface tilted at β angle and installed facing γ azimuth angle, receives Global Irradiance $GI_{\beta\gamma}$, which could be analyzed to direct $DBI_{\beta\gamma}$, diffuse $DI_{\beta\gamma}$ and reflected from

the ground $RGI_{\beta\gamma}$ components. A graphical representation of the relations between the irradiance components is provided in Figure 2.

$$GI_{\beta\gamma} = DBI_{\beta\gamma} + DI_{\beta\gamma} + RGI_{\beta\gamma} \quad (1)$$

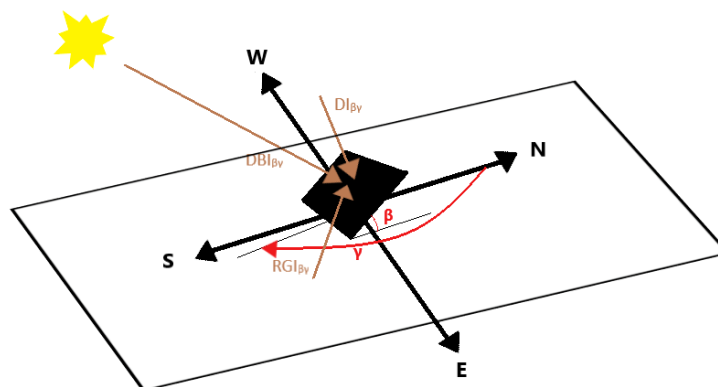


Figure 2. Graphical Presentation of the β tilt angle and γ azimuthal angle, alongside of Diffuse, Direct Beam and Reflective components of received solar irradiance.

Various approaches have been suggested to model the incident $GI_{\beta\gamma}$, which are estimating the diffuse component. The simplest approach is to assume that the propagation of irradiance is isotropic. Anisotropic models also consider the components of diffuse irradiance coming from circumsolar and the horizon.

Four different irradiance models have been evaluated in order to estimate the incident irradiance to inclined surfaces. These models are accordingly ISO [32], Hay [33], Reindl [34] and Perez [35]. The formulas used by these models are presented in Appendix A. The main difference between them is that ISO model assumes isotropical irradiance, Hay and Reindl models also estimate irradiance from circumsolar and Perez model is the only one adding diffuse irradiance from the horizon. Four cities (Nicosia, Athens, Bergen and Reykjavik) were selected to perform the evaluation in the whole dataset.

We are not aware of any available ground-based measurements at different tilt angles in order to validate the results. A similar study performed in Athens [8] showed very small deviations between the results, with Hay showing the best agreement with tilted pyranometers. Other studies [36,37], found the Perez model to outperform the others in Reunion island and Denmark, accordingly. Chinchilla [26] suggested that Perez model had the best results when validated against BSRN stations.

Finally, the selection of the surface albedo plays a crucial role in calculating $RGI_{\beta\gamma}$. For lower latitudes a constant isotropic model was used, which suggests a constant value of $\rho = 0.2$. Snow is the main factor that causes significant variations from the constant value. A simple approach in this case is to use an isotropic seasonal model, which changes monthly according to climatological conditions and calculated by the formula found at [38]. We have used this model for cities with latitudes higher than 50° , aiming to reduce the error introduced by snow covered conditions.

3. Results

3.1. Model Comparison

In order to compare the models, we have calculated for each city the GI at tilt angles from 1° to 90° with 1° step, for all time steps. The comparison is performed for four cities, two in Southern and two in Northern Europe, in order to minimize local effects. The total estimated received energy per day, for each angle for the whole period and then the mean values are calculated. Finally, we estimated the tilt angle that had the highest daily energy outcome for each city. Results of our assessment are presented in Figure 3 and Tables 1 and 2. Perez model estimates higher energy output than the other

three models, which is partially explained by being the only one adding the horizon diffuse irradiance component. When inclination is close to 0° , the differences between the models are almost zero. This is explained by the fact that the horizontal irradiance is the main component at these inclinations, which is also the input to the models. Hay and Reindl models have almost the same results in angles lower than 60° but diverge significantly when the inclination is closest to the vertical. In addition, the ISO model estimates the lowest irradiance values, in all cases, when inclination is lower than 60° . Standard deviation of optimal angle is between 1.25° and 1.78° and the one of daily energy output $0.05\text{--}0.09\text{ kWh/m}^2/\text{day}$. Higher deviation of optimum angle is found in Reykjavik, where Perez model provides a more than 2° higher angle than any other model, and this should be linked with the diffuse irradiance from the horizon, which is only considered at this model. On southern latitudes models' estimations converge on optimal tilt angle. On the other hand, in terms of absolute energy values at these latitudes the differences are higher than in Northern areas. Perez models seem to constantly provide higher irradiance compared to the others, while Hay model has the lowest values in northern areas and ISO in southern. Reindl model is the one closest to the mean value of all four models, both in terms of mean energy and optimum tilt angle, in most cases, although with very slight differences from Hay. Hence, we will use Reindl model for the rest of the study, clarifying that there is an uncertainty entered by the selection of diffuse irradiance model, in the order of 0.7° in terms of inclination angle and $0.04\text{ kWh/m}^2/\text{day}$ in terms of energy output. This uncertainty was calculated by the mean difference of Reindl's model to other three for all cities.

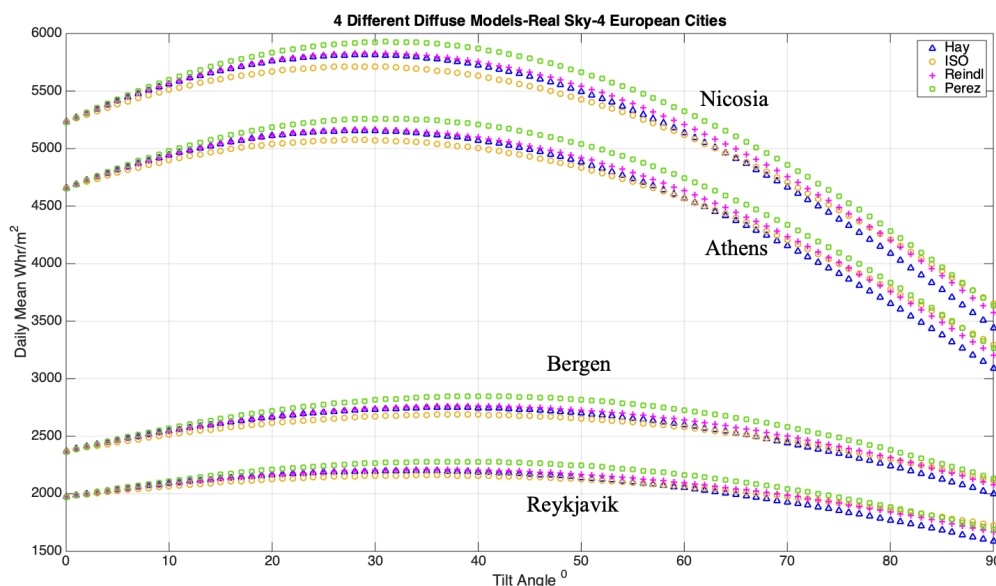


Figure 3. Mean Daily Total Radiation for Athens, Nicosia, Bergen and Reykjavik, for inclinations of 0° to 90° as calculated by different models.

Table 1. Mean Optimum Angle for test cities as calculated with each model, the mean and standard deviation σ for each city as calculated from model's prognosis.

Optimum Angle	Hay	ISO	Reindl	Perez	Mean	σ
Nicosia	28.8	28.47	29.67	31.27	29.55	1.25
Athens	28.33	28.27	29.13	30.87	29.15	1.21
Bergen	37.07	38.13	38.8	40.40	38.60	1.40
Reykjavik	33.53	35.27	35.67	37.87	35.59	1.78

Table 2. Daily Energy outcome at the suggested optimum tilt angle for test cities as calculated with each model, the mean and standard deviation σ for each city as calculated from model's prognosis.

kWh/m ² /Day	Hay	ISO	Reindl	Perez	Mean	σ
Nicosia	5.81	5.71	5.83	5.93	5.82	0.09
Athens	5.15	5.08	5.17	5.26	5.17	0.07
Bergen	2.75	2.69	2.76	2.85	2.76	0.07
Reykjavik	2.20	2.16	2.21	2.28	2.21	0.05

3.2. Optimum Angle per City

We have calculated the optimal tilt angle, that provides the highest energy outcome year-round, for each city, as estimated by the full historical hourly data. For these calculations the Reindl model has been used and the GI_{β} has been estimated for the whole dataset, for β in the range 1° to 90° with 1° step. Then, the sum of received irradiance at each β for the whole period, was calculated and the β with the higher value for each city was selected as optimal. The results are presented at Table 3, alongside with mean CMF and AOD at 550 nm for each city. The difference between latitude and optimal tilt angle is wider to the northern areas. This behavior should be explained mainly by the increase of cloud coverage at these areas. At southern areas, the tilt angles differences are smaller, because the latitude suggest closer to horizontal tilt and cloud coverage is lower. However, these areas receive more sunlight, hence these smaller variations could lead to significant energy gains. CMF is generally lower as latitude increases, at least in the region of Europe and North Africa. AOD on the other hand has higher values in lower latitudes in this region, which is explained by the dominance of Saharan dust on high aerosol episodes in the area [39,40].

Table 3. Latitude and Longitude of Cities used in the study, alongside with mean CMF and AOD and the calculated optimum tilt angle β for the period 2005–2019.

City	Country	Lat	Long	β_{opt}	<CMF>	<AOD>
Tamanrasset	Algeria	22.78	5.51	21	0.869	0.312
Aswan	Egypt	24.09	32.89	23	0.914	0.310
Cairo	Egypt	30.03	31.24	25	0.863	0.282
Marrakesh	Morocco	31.63	−7.98	28	0.841	0.205
Nicosia	Cyprus	35.17	33.36	29	0.840	0.245
Valletta	Malta	35.89	14.51	29	0.835	0.238
Athens	Greece	37.98	23.72	29	0.784	0.222
Madrid	Spain	40.43	−3.70	31	0.783	0.140
Thessaloniki	Greece	40.65	22.92	31	0.744	0.232
Rome	Italy	41.88	12.47	32	0.783	0.197
Bucharest	Romana	44.44	26.08	32	0.683	0.224
Ljubljana	Slovenia	46.05	14.50	32	0.664	0.196
Paris	France	48.94	2.41	32	0.642	0.178
Kyiv	Ukraine	50.41	30.50	33	0.641	0.190
Warsaw	Poland	52.23	21.00	33	0.616	0.192
Berlin	Germany	52.52	13.37	33	0.623	0.180
Dublin	Ireland	53.34	−6.28	34	0.636	0.170

Table 3. Cont.

City	Country	Lat	Long	β_{opt}	$\langle CMF \rangle$	$\langle AOD \rangle$
Copenhagen	Denmark	55.71	12.54	34	0.626	0.161
Moscow	Moscow	55.8	37.59	34	0.578	0.176
Riga	Lithuania	56.95	24.11	35	0.625	0.158
Stockholm	Sweden	59.27	18.02	35	0.633	0.137
Helsinki	Finland	60.19	24.93	36	0.565	0.137
Bergen	Norway	60.37	5.32	37	0.587	0.145
Reykjavik	Iceland	64.16	−21.95	37	0.511	0.138
Alvsbyn	Norway	65.68	20.99	40	0.593	0.101

At Figure 4, we present the mean monthly ratio between GI_{β} and GHI , which represents the gain/loss of tilted surface, compared with a horizontal one. Both the cases of tilt angle of latitude and the optimal as calculated above are demonstrated. In addition, monthly values for all 25 cities are implemented at the plot. In wintertime, the relative gain is higher, but also the spread of ratios among cities. In general, areas with very low cloud coverage—at southern areas—have less relative gain, although the absolute values are higher. Areas at the north, where sunshine duration is very low during winter seem to have the biggest relative benefit, since the cloud coverage is almost permanent at this season. In spring and autumn, the relative gains of optimal instead of latitude angle are more obvious. In addition, at these seasons, the relative benefit of higher latitudes is larger than the southern ones. More interesting is that in summer months, almost in all cities, both setups provide less energy than the horizontal surface. This is explained because the Solar Zenith Angle of the periods of peak GHI are closest to 0 than to latitude in all cases, hence the horizontal surface receives more irradiance. The biggest disadvantage of having a fixed angle year-round is that during summer months the solar potential is not fully exploited, but summing the whole year, it is the preferred setup. Previous work (e.g., [8]) have investigated the possibility of 2 or 4 changes of the fixed angle, around the year in order to increase the benefits.

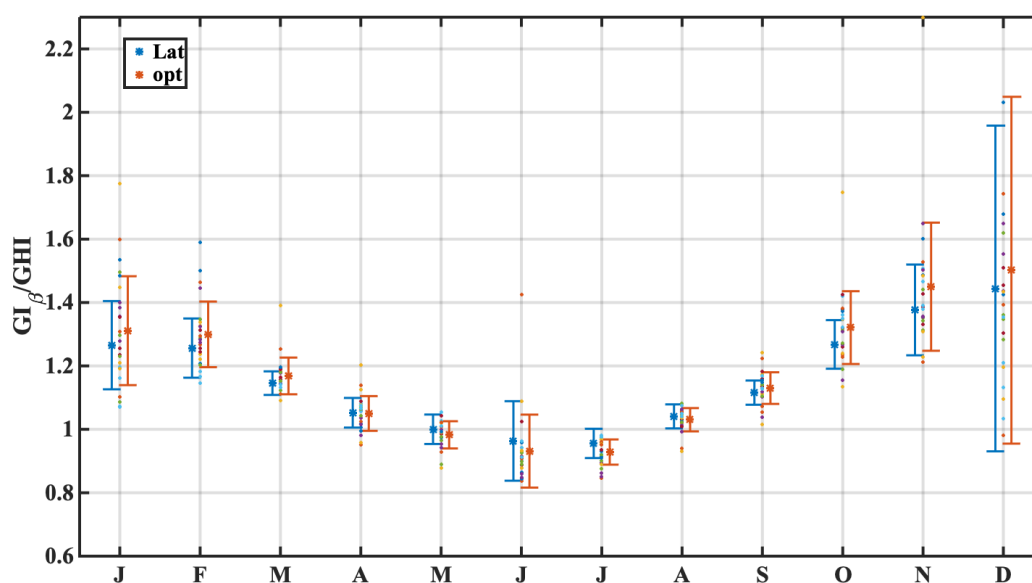


Figure 4. Ratio of GI_{β} on inclined surface to horizontal one, for each month. Mean value for each month for $\beta =$ Latitude and $\beta =$ optimum angle, along with error bars representing the 1σ standard deviation of ratios for each month. Small points are all 25 cities ratios for each month.

Clouds are the main the factor that act on the propagation of radiation and alter the most efficient tilt angle. By observing that in the region of study, these are almost proportional to geographical latitude, we decided to test the possibility of using latitude as a proxy of these factors. Our aim is to extract by regression an equation that could be applied in places where no climatological information is available on clouds and aerosols. The equation should be in the form of:

$$\beta_{opt} = f(\varphi) \quad (2)$$

And we have plotted optimum tilt angle (with $\pm 1\sigma$ error bars) against the latitude for all 25 cities (Figure 5a). The linear regression forecast equation is shown on the Figure and the extracted linear polynomial is:

$$\beta_{opt} = 0.34 \times \varphi + 15.72 \quad (3)$$

The goodness of fit is satisfactory with $R^2 = 0.937$ and $RMSE = 1.81$. Hence, this equation could be in use.

But since the normal in actual installations is to use the latitude of the area as the tilt angle, we decided to parameterize an equation as the difference of the latitude and the optimum angle, in an equation of the form:

$$\varphi - \beta_{opt} = f(\varphi) \quad (4)$$

Which is calculated by the corresponding plot at Figure 5b and the calculated polynomial is:

$$\varphi - \beta_{opt} = 0.65 \times \varphi - 15.72 \quad (5)$$

In this case, the goodness of fit is better, with $R^2 = 0.945$ and $RMSE = 1.71$. The quantity $\varphi - \beta$ that we parameterized, is the component of the tilt angle that is depended on atmospheric conditions, since the astronomical calculations suggest the latitude as preferred tilt angle for clear skies conditions.

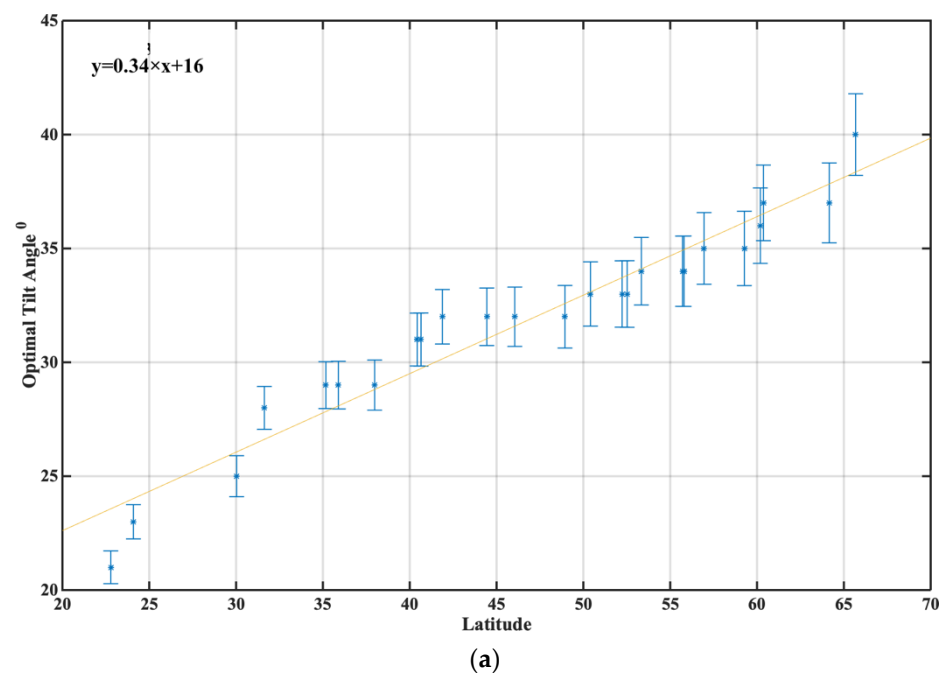


Figure 5. Cont.

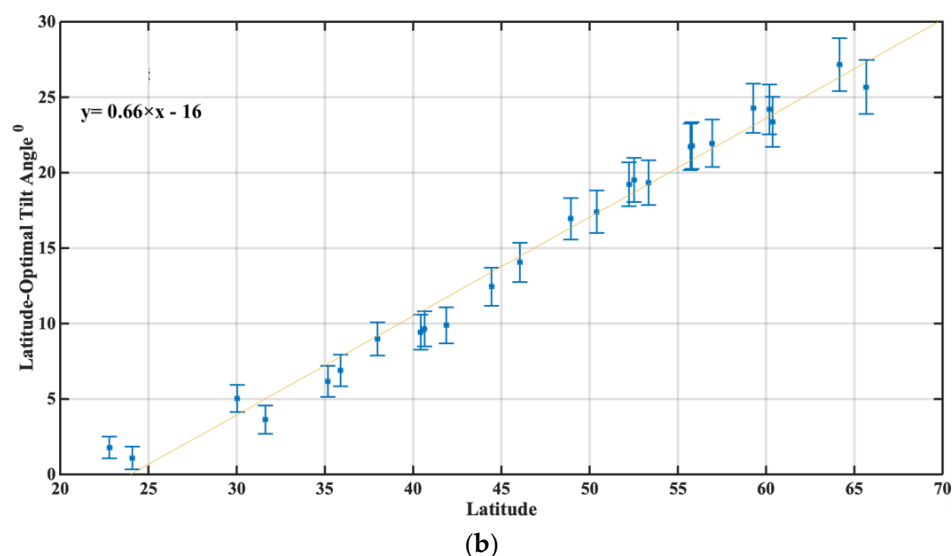


Figure 5. Optimum tilt angle with 1σ against latitude for all cities and corresponding linear regression (a). Difference of Latitude and Optimum tilt angle with 1σ against latitude for all cities and corresponding linear regression (b).

We can notice in both plots that Tamanrasset has the largest distance to the regression line ($\sim 3^\circ$), which leads to doubt on applying these equations in subtropical areas. In general, with both approaches the results are adequate, keeping in mind that latitude is just a proxy of the actual conditions and that these relations could not be applied everywhere, since not all places show this latitudinal dependence—due to different cloud patterns in other regions.

3.3. Cloud Effect

In this section we aim to quantify the effect of clouds on the selection of the most efficient tilt angle. Cloud presence is the main factor that modifies the *GI* and makes tilt angles closer to the horizontal more efficient. Clouds effect is greater than any other atmospheric component and since aerosols and gases are included the clear sky *GHI* calculation, *CMF* calculated is an adequate measure for the effect of clouds.

At Figure 6, the relation of the difference of tilt angle in respect to *CMF* is shown. A parameterization in the form of:

$$\varphi - \beta_{opt} = f(CMF) \quad (6)$$

is exported from this data set by second degree polynomial regression as:

$$\varphi - \beta_{opt} = 30.24 \times CMF^2 - 112.16 \times CMF + 78.12 \quad (7)$$

Statistics of this fit show $R^2 = 0.962$ and $RMSE = 1.48$. Thus, we should interpret that this approach is a more accurate representation of the actual state. For cities with lower cloud coverage—which are also at lower latitudes—change of tilt angle is more accurately predicted, except for Tamanrasset, where desert dust aerosols add some variation to the calculations. Bucharest and Ljubljana show lower change of the tilt angle than expected from the regression of *CMF* of the area. Finally, at Stockholm the actual change is more than 5° greater than predicted from the *CMF* equation (19.4° instead of 24.7°), where the latitude parameterization provided a more accurate estimation for the area (24.1°).

The uncertainty due to the selection of diffuse irradiance model should be considered here, since variations between them have different effect according to the actual climatological cloud properties in each area. Since, Reindl model is used, as discussed in Section 3.1, the simulation of the diffuse angle could be in the range of $\pm 0.7^\circ$ for the tilt angle. It

should be highlighted that other factors for defining the optimal angle (mainly aerosols) are ignored at this approach and could be attributed for the deviations.

We have calculated the differences of mean daily energy output for areas where the simulations and the regression show large deviations. For Stockholm the difference is 0.02 kWh/m²/day, for Ljubljana is 0.04 kWh/m²/day, for Bucharest is 0.03 kWh/m²/day and for Tamanrasset is 0.01 kWh/m²/day.

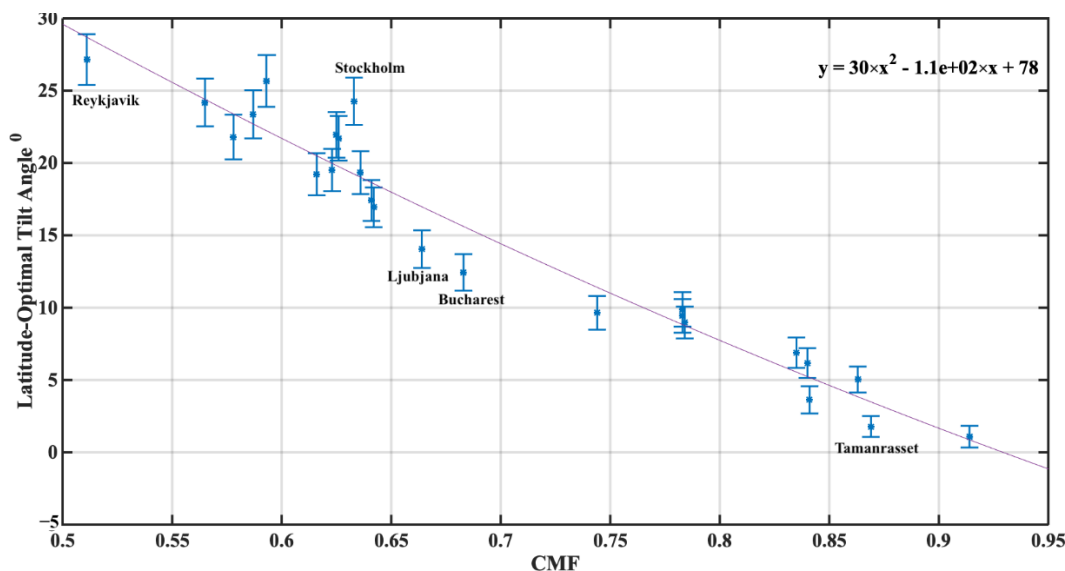


Figure 6. Optimum tilt angle with 1 σ against latitude for all cities and corresponding linear regression.

3.4. Energy/Financial Profits

Figure 7 shows the energy and financial profits of the optimal tilt angle (OPT) as compared to the latitudinal tilt angle (LAT) for a 1 MWp capacity PV system, hypothetically installed in the 25 cities in Europe and North Africa. For the PV and financial calculations, the methodology described in numerous studies [41–44] was followed in brief, for the PV calculations the crystalline silicon was assumed as the most popular technology worldwide [45] accompanied by a research-cell efficiency of 13–26% [46]. By including realistic operating conditions of the PV infrastructure, the total efficiency value falls to an average level of almost 12%. The combined losses are of the order of 29% and are related to external and self-shading [47] (to avoid the self-shading a spatial coverage close to 80% is recommended for tilted panels at horizontal rooftops), as well as thermal, reflection, cables and inverter losses, but also dust and dirt deposition [48]. For the simulation of the above energy production technicalities the Photovoltaic Geographic Information System (PVGIS) was used [49]. To this direction, the cities were sorted by the corresponding solar energy potential difference between the optimal and the latitude tilt angles (blue line in Figure 7). The above solar energy potential values are translated also to percentage differences in the range of 0–2.37% (blue bars in Figure 7) indicating the overall improvement from the selection of the optimum tilt angle. The result is dependent on the average cloudiness (see Table 3) of the cities with the lowest differences occurring in the North African locations and southern Europe (e.g., Cairo, Tamanrasset, Aswan, Athens, Nicosia) and the highest differences at higher latitudes, i.e., 23 kWh/m² in Alvsbyn (977 and 1000 kWh/m² for latitude and optimal angles, respectively). For the estimation of the financial profit, the feed-in tariffs (FIT) retrieved from the European Environment Agency (<https://www.eea.europa.eu/>) (accessed on 1 April 2022) were incorporated in the calculations, indicating the policy making dimension into the PV technology promotion and penetration into society. The above statement is reflected in the wide price range which is from 0.019 to 0.19 euro/kWh with the lowest FIT occurring in cities such as Alvsbyn, Stockholm, Copenhagen, Aswan

and Cairo (<0.04 euro/kWh) and the highest prices in Madrid, Rome, Valletta, Kyiv, Warsaw and Dublin (>0.12 euro/kWh). Especially in Dublin, the revenue difference is close to 2750 euro for 1 MWp capacity on an annual basis, making the optimal angle identification a key parameter for the financial profit optimization.

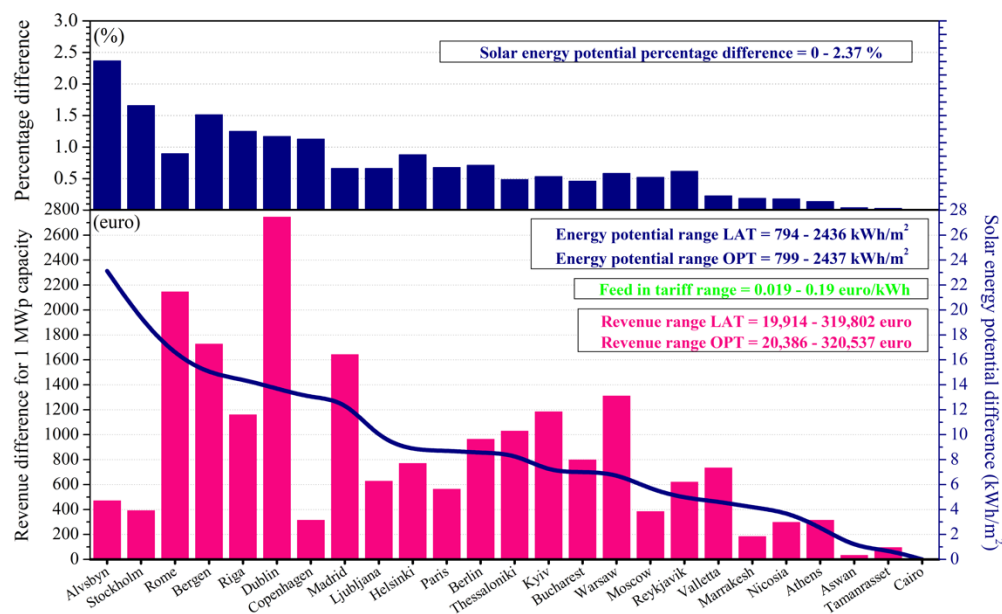


Figure 7. Annual solar energy potential and revenue (for 1 MWp capacity) differences and percentage differences for all cities included in the study, between latitude and optimum tilt angle installations.

4. Discussion

The validity of the results is strongly dependent on the data set used for the calculations. Historic assimilated data from CAMS database were used in this study, for 15 years. Variations in atmospheric conditions from year to year, would affect the final outcome. 15 years is a period that some outliers in cloud coverage would be detected but could only be considered as representative for this time period. The pioneer work of Jacobson [24], used typical meteorological years from PVWatts database for places all over the globe, which was calculated using data from the 1960–1990 period. PVWatts uses the Bird Simple Spectral Model [50], which uses the isotropy assumption for calculating incident irradiance on titled surfaces. 10 Cities presented in that study, are common with present work (including Vatican City in Rome metropolitan area and Rabat, Malta which is located less than 10 km from Valetta). For 3 cities the exact same optimum tilt angle is estimated in Jacobson and our study and another five have differences of less than 2°. For Stockholm and Reykjavik high differences are found between the studies—6° in both cases. Factors that could explain these differences could be the different time periods for the calculations, differences in cloud conditions, the circumsolar radiation ignored by the Bird Model and the surface albedo in snow covered areas. It should be highlighted that in many areas the atmospheric pollution (including aerosols) had changed between the periods covered by PVWatts and CAMS datasets [51,52]. Additionally, the exact optimal tilt angles for all 25 cities included in the present study, were calculated using the global equation proposed by Jacobson and are shown in Figure 8. The mean difference is 1.9° with higher difference found at Reykjavik which is 3.7°. Generally, Jacobson equation estimates higher optimal angles than the ones found on this study, with the area of latitudes above 45° having the biggest deviations. This behavior is partially explained by the curvature of the 3rd order polynomial selected on Jacobson study, which deviates more at these latitudes. Nevertheless, the further north city of Alsbjorn show difference of 0.9°, which is lower than other Northern cities. Cloud coverage is the reason for this behavior, since in this area, the cloud coverage is lower than other areas with latitudes above 60°. These deviations point out the difficulty of having a

global parameterization for optimal tilt angle in respect to latitude, since cities with same latitude could have a large deviation in meteorological conditions and more regional scales should be preferred for these calculations. However, the parameterization in respect to cloud coverage, show a potential for application in larger scales, since it is the main variable causing the modification of the optimal angle.

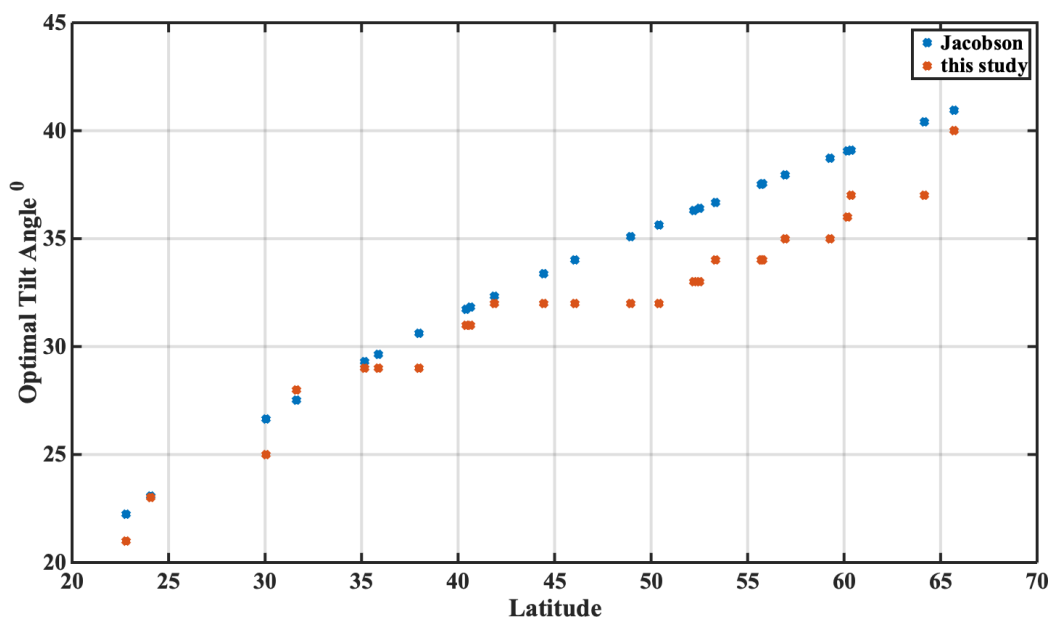


Figure 8. Optimal Tilt angle for the 25 Cities used in the present study, as calculated by Reindl model [31] (red) and as estimated by the equation proposed by Jacobson [24] (blue).

Other issues that should be considered when selecting a fixed angle PV installation, such natural rain washing of dust on the panels, which is more effective at higher inclinations. Potential trends of atmospheric pollution and/or cloudiness for the next decades should be considered before selecting inclinations for PV with long lifetime. Finally, the exact financial costs of installing solar tracking systems and compared to the optimum fixed angle selection and balance the energy benefits of each solution, including the seasonality.

5. Conclusions

The preferred tilt angle for surfaces in order to maximize received solar irradiance have been studied. 25 cities in Europe and North Africa were selected and 15 years of irradiance data from CAMS were exploited. Four different diffuse irradiance models were tested, and we have selected to carry out the study using Reindl model with isotropic constant albedo at lower latitudes and isotropic seasonal albedo for regions above 50° . The uncertainty introduced by the selection of the model has been estimated as 0.7° tilt angle and $0.04 \text{ kWh/m}^2/\text{day}$ energy output.

The optimum tilt angle that provides the maximum intake of solar irradiance year-round has been estimated for each city. The difference between the latitude and the optimum tilt angle has been parameterized in respect to latitude and *CMF* and corresponding equations are presented in order to be applied by users in other areas. Agreement of the proposed equations—quantified as R^2 —was found between 0.93 and 0.97. Better statistics for the parameterization using the *CMF*, but with some regions having considerable differences. These equations could be employed anywhere in the same region to select the optimal tilt angle. In general, installations at higher latitudes could benefit from considerably lower tilt angle than the latitude. Higher cloud coverage also leads to optimal tilt angles closer to the horizontal. At middle latitudes the absolute differences of the tilt angles were smaller but lead to considerable energy benefits.

From an economic point of view, the selection of the optimum tilt angle is able to result in an average annual increase in revenue reaching almost 2800 euro per 1 MWp of capacity installed as compared to the latitudinal tilt. At the same time, the national strategies concerning the running feed-in tariffs form a critical parameter that affects the revenue streams depending on solar energy production and the subsequent profitability margins.

Differences from the global equation for optimal tilt angle proposed by Jacobson [24] were investigated and found that the equation overestimates more than 2° in European regions with latitude higher than 45°. Reasons for those deviations are found in the selection of different models and training datasets.

When planning new PV installations, it is rare to have years long ground-based measurements of solar irradiance in the area. In most cases databases such as CAMS or PVWatts are the best tool available, but it should be considered that they are reanalysis models based on historical satellite retrievals, hence it differs from actual solar measurements. However, studies [53–55] showed that these differences can be considered reasonable with no systematic deviations related with latitude. These tools are the proper way to approach the prognosis for the optimal tilt angle in a region for the next decades.

In summary, when considering fixed tilt installations, the cloud (and aerosol) climatology of the area should be taken into account alongside with estimations for the next decades. Small variations of datasets or tools used, could lead to high financial gains/loses. Future research should focus on the homogenization of the procedures in order to provide accurate and accessible tools to anyone planning to exploit solar energy potential.

Author Contributions: Conceptualization, I.-P.R. and S.K.; methodology, I.-P.R., S.K. and P.K.; software, A.M. and I.-P.R.; formal analysis, A.M. and I.-P.R.; investigation, A.M., I.-P.R. and P.K.; resources, S.K.; data curation, A.M. and I.-P.R.; writing—original draft preparation, I.-P.R. and P.K.; writing—review and editing, S.K. and P.K.; visualization, A.M., P.K. and I.-P.R.; supervision, S.K. and I.-P.R.; funding acquisition, S.K. All authors have read and agreed to the published version of the manuscript.

Funding: This research received no external funding.

Data Availability Statement: All CAMS data are available freely for download Copernicus portal <http://atmosphere.copernicus.eu/> (accessed on 1 April 2022) and the SODA portal <http://www.soda-pro.com/web-services/radiation/cams-radiation-service> (accessed on 1 April 2022).

Acknowledgments: We acknowledge the support of European Commission project EuroGEO e-shape (grant agreement No. 820852) and by the Eiffel project (grant agreement No. 101003518).

Conflicts of Interest: The authors declare no conflict of interest.

Appendix A

Relations used for calculating in:

ISO

$$DI_{\beta\gamma ISO} = DHI \cdot \frac{(1 + \cos\beta)}{2} \quad (A1)$$

Hay

$$DI_{\beta\gamma HAY} = DHI \cdot \left[\left(1 - \frac{BHI}{I_0}\right) \cdot \frac{(1 + \cos\beta)}{2} + \frac{BHI}{I_0} \cdot \frac{\cos(\theta)}{\cos(\theta_z)} \right] \quad (A2)$$

Reindl

$$DI_{\beta\gamma Reindl} = DHI \cdot \left[\left(1 - \frac{BHI}{I_0}\right) \cdot \frac{(1 + \cos\beta)}{2} \cdot \left(1 + f \cdot \sin^3\left(\frac{\beta}{2}\right)\right) + \left(\frac{BHI}{I_0} \cdot \frac{\cos(\theta)}{\cos(\theta_z)}\right) \right] \quad (A3)$$

$$f = 1 - \left(\frac{DHI}{GHI}\right)^2 \quad (A4)$$

Perez

$$DI_{\beta\gamma\text{PEREZ}} = DHI \cdot \left[(1 - F_1) \cdot \left(\frac{1 + \cos\beta}{2} \right) + F_1 \cdot \left(\frac{\alpha_0}{\alpha_1} \right) + F_2 \cdot \sin\beta \right] \quad (\text{A5})$$

where α_0 and α_1 are calculated as:

$$\alpha_0 = \max[0, \cos\theta] \quad (\text{A6})$$

$$\alpha_1 = \max[\cos 85, \cos\theta_z] \quad (\text{A7})$$

F_1 and F_2 are estimated by parameter ε and Δ as:

$$F_1 = \max[0, F_{11} + F_{12} \cdot \Delta + (\pi/180) \cdot \theta_z \cdot F_{13}] \quad (\text{A8})$$

$$F_2 = [F_{11} + F_{22} \cdot \Delta + (\pi/180) \cdot \theta_z \cdot F_{23}] \quad (\text{A9})$$

where:

$$\Delta = \frac{m \cdot DHI}{I_0} \quad (\text{A10})$$

$$m = \frac{1}{\sin(El) + a(El + b)^{-c}} \quad (\text{A11})$$

El is solar elevation ($^\circ$) and a , b , c are constants, used as 0.15, 3.885, 1.253. Clarity index ε is calculated:

$$\varepsilon_i = \frac{\left(\frac{DHI + DNI}{DHI} \right) + 5.535 \cdot 10^{-6} \cdot \theta_z^3}{1 + 5.535 \cdot 10^{-6} \cdot \theta_z^3} \quad (\text{A12})$$

where θ_z .

Through ε and the table provided at [33] the parameters F_{11} , F_{12} , F_{13} , F_{22} , F_{23} are calculated and finally the diffuse irradiance $DI_{\beta\gamma\text{Perez}}$.

References

- Malm, A. *Fossil Capital: The Rise of Steam-Power and the Roots of Global Warming*; Verso: London, UK; New York, NY, USA, 2016; ISBN 978-1-78478-129-3.
- Kåberger, T. Progress of Renewable Electricity Replacing Fossil Fuels. *Glob. Energy Interconnect.* **2018**, *1*, 48–52. [CrossRef]
- Shukla, P.R.; Skea, J.; Slade, R.; Al Khourdajie, A.; van Diemen, R.; McCollum, D.; Pathak, P.; Some, S.; Vyas, P.; Fradera, R.; et al. IPCC, 2022: Climate Change 2022: Mitigation of Climate Change. In *Contribution of Working Group III to the Sixth Assessment Report of the Intergovernmental Panel on Climate Change*; IPCC: Geneva, Switzerland, 2022.
- Renewables Global Futures Report: Great Debates towards 100% Renewable Energy*; REN21: Paris, France, 2017.
- IEA (2021), Renewables 2021. Available online: <https://www.iea.org/reports/renewables-2021> (accessed on 1 May 2022).
- Mehler, E.D.; Zervas, P.L.; Sarimveis, H.; Palyvos, J.A.; Markatos, N.C. Determination of the Optimal Tilt Angle and Orientation for Solar Photovoltaic Arrays. *Renew. Energy* **2010**, *35*, 2468–2475. [CrossRef]
- Kaldellis, J.; Zafirakis, D. Experimental Investigation of the Optimum Photovoltaic Panels' Tilt Angle during the Summer Period. *Energy* **2012**, *38*, 305–314. [CrossRef]
- Raptis, P.I.; Kazadzis, S.; Psiloglou, B.; Kouremeti, N.; Kosmopoulos, P.; Kazantzidis, A. Measurements and Model Simulations of Solar Radiation at Tilted Planes, towards the Maximization of Energy Capture. *Energy* **2017**, *130*, 570–580. [CrossRef]
- Kocer, A.; Yaka, I.F.; Sardogan, G.T.; Gungor, A. Effects of Tilt Angle on Flat-Plate Solar Thermal Collector Systems. *Curr. J. Appl. Sci. Technol.* **2015**, *9*, 77–85. [CrossRef]
- Tong, X.; Sun, Z.; Sigrimis, N.; Li, T. Energy Sustainability Performance of a Sliding Cover Solar Greenhouse: Solar Energy Capture Aspects. *Biosyst. Eng.* **2018**, *176*, 88–102. [CrossRef]
- Kacira, M.; Simsek, M.; Babur, Y.; Demirkol, S. Determining Optimum Tilt Angles and Orientations of Photovoltaic Panels in Sanliurfa, Turkey. *Renew. Energy* **2004**, *29*, 1265–1275. [CrossRef]
- Lave, M.; Kleissl, J. Optimum Fixed Orientations and Benefits of Tracking for Capturing Solar Radiation in the Continental United States. *Renew. Energy* **2011**, *36*, 1145–1152. [CrossRef]
- Rowlands, I.H.; Kemery, B.P.; Beausoleil-Morrison, I. Optimal Solar-PV Tilt Angle and Azimuth: An Ontario (Canada) Case-Study. *Energy Policy* **2011**, *39*, 1397–1409. [CrossRef]
- Díez-Mediavilla, M.; Rodríguez-Amigo, M.; Dieste-Velasco, M.; García-Calderón, T.; Alonso-Tristán, C. The PV Potential of Vertical Façades: A Classic Approach Using Experimental Data from Burgos, Spain. *Sol. Energy* **2019**, *177*, 192–199. [CrossRef]

15. Wang, M.; Mao, X.; Gao, Y.; He, F. Potential of Carbon Emission Reduction and Financial Feasibility of Urban Rooftop Photovoltaic Power Generation in Beijing. *J. Clean. Prod.* **2018**, *203*, 1119–1131. [CrossRef]
16. Mohammad, S.T.; Al-Kayiem, H.H.; Aurybi, M.A.; Khelif, A.K. Measurement of Global and Direct Normal Solar Energy Radiation in Seri Iskandar and Comparison with Other Cities of Malaysia. *Case Stud. Therm. Eng.* **2020**, *18*, 100591. [CrossRef]
17. Nassar, Y.F.; Hafez, A.A.; Alsadi, S.Y. Multi-Factorial Comparison for 24 Distinct Transposition Models for Inclined Surface Solar Irradiance Computation in the State of Palestine: A Case Study. *Front. Energy Res.* **2020**, *7*, 163. [CrossRef]
18. Serrano-Guerrero, X.; Cantos, E.; Feijoo, J.-J.; Barragán-Escandón, A.; Clairand, J.-M. Optimal Tilt and Orientation Angles in Fixed Flat Surfaces to Maximize the Capture of Solar Insolation: A Case Study in Ecuador. *Appl. Sci.* **2021**, *11*, 4546. [CrossRef]
19. Darhmaoui, H.; Lahjouji, D. Latitude based model for tilt angle optimization for solar collectors in the Mediterranean region. *Energy Procedia* **2013**, *42*, 426–435. [CrossRef]
20. Chang, Y.-P. Optimal Design of Discrete-Value Tilt Angle of PV Using Sequential Neural-Network Approximation and Orthogonal Array. *Expert Syst. Appl.* **2009**, *36*, 6010–6018. [CrossRef]
21. Nicolás-Martín, C.; Santos-Martín, D.; Chinchilla-Sánchez, M.; Lemon, S. A Global Annual Optimum Tilt Angle Model for Photovoltaic Generation to Use in the Absence of Local Meteorological Data. *Renew. Energy* **2020**, *161*, 722–735. [CrossRef]
22. Salata, F.; Ciancio, V.; Dell’Olmo, J.; Golasi, I.; Palusci, O.; Coppi, M. Effects of Local Conditions on the Multi-Variable and Multi-Objective Energy Optimization of Residential Buildings Using Genetic Algorithms. *Appl. Energy* **2020**, *260*, 114289. [CrossRef]
23. Petrović, E.; Jović, M.; Nikolić, V.; Mitrović, D.; Laković, M. Particle Swarm Optimization for the Optimal Tilt Angle of Solar Collectors. In Proceedings of the Sixteenth Symposium on Thermal Science and Engineering of Serbia, Sokobanja, Serbia, 22–25 October 2013.
24. Jacobson, M.Z.; Jadhav, V. World Estimates of PV Optimal Tilt Angles and Ratios of Sunlight Incident upon Tilted and Tracked PV Panels Relative to Horizontal Panels. *Sol. Energy* **2018**, *169*, 55–66. [CrossRef]
25. NREL (National Renewable Energy Laboratory), 2017. PV Watts Calculator. Available online: <http://Pvwatts.Nrel.Gov> (accessed on 4 November 2017).
26. Chinchilla, M.; Santos-Martín, D.; Carpintero-Rentería, M.; Lemon, S. Worldwide Annual Optimum Tilt Angle Model for Solar Collectors and Photovoltaic Systems in the Absence of Site Meteorological Data. *Appl. Energy* **2021**, *281*, 116056. [CrossRef]
27. Oumbe, A.; Qu, Z.; Blanc, P.; Lefèvre, M.; Wald, L.; Cros, S. Decoupling the Effects of Clear Atmosphere and Clouds to Simplify Calculations of the Broadband Solar Irradiance at Ground Level. *Geosci. Model Dev.* **2014**, *7*, 1661–1669. [CrossRef]
28. de Miguel, A.; Bilbao, J.; Aguiar, R.; Kambezidis, H.; Negro, E. Diffuse Solar Irradiance Model Evaluation in the North Mediterranean Belt Area. *Sol. Energy* **2001**, *70*, 143–153. [CrossRef]
29. Kopp, G.; Lean, J.L. A new, lower value of total solar irradiance: Evidence and climate significance. *Geophys. Res. Lett.* **2011**, *38*. [CrossRef]
30. Parisi, A.V.; Turnbull, D.J.; Turner, J. Calculation of cloud modification factors for the horizontal plane eye damaging ultraviolet radiation. *Atmos. Res.* **2007**, *86*, 278–285. [CrossRef]
31. Lefèvre, M.; Oumbe, A.; Blanc, P.; Espinar, B.; Gschwind, B.; Qu, Z.; Wald, L.; Schroedter-Homscheidt, M.; Hoyer-Klick, C.; Arola, A.; et al. McClear: A New Model Estimating Downwelling Solar Radiation at Ground Level in Clear-Sky Conditions. *Atmos. Meas. Tech.* **2013**, *6*, 2403–2418. [CrossRef]
32. Liu, B.; Jordan, R. Daily Insolation on Surfaces Tilted towards Equator. *ASHRAE J.* **1961**, *10*.
33. Hay, J.E. Calculation of Monthly Mean Solar Radiation for Horizontal and Inclined Surfaces. *Sol. Energy* **1979**, *23*, 301–307. [CrossRef]
34. Reindl, D.T.; Beckman, W.A.; Duffie, J.A. Evaluation of Hourly Tilted Surface Radiation Models. *Sol. Energy* **1990**, *45*, 9–17. [CrossRef]
35. Perez, R.; Ineichen, P.; Seals, R.; Michalsky, J.; Stewart, R. Modeling Daylight Availability and Irradiance Components from Direct and Global Irradiance. *Sol. Energy* **1990**, *44*, 271–289. [CrossRef]
36. David, M.; Lauret, P.; Boland, J. Evaluating Tilted Plane Models for Solar Radiation Using Comprehensive Testing Procedures, at a Southern Hemisphere Location. *Renew. Energy* **2013**, *51*, 124–131. [CrossRef]
37. Tian, Z.; Perers, B.; Furbo, S.; Fan, J.; Deng, J.; Dragsted, J. A Comprehensive Approach for Modelling Horizontal Diffuse Radiation, Direct Normal Irradiance and Total Tilted Solar Radiation Based on Global Radiation under Danish Climate Conditions. *Energies* **2018**, *11*, 1315. [CrossRef]
38. Gueymard, C. Critical Analysis and Performance Assessment of Clear Sky Solar Irradiance Models Using Theoretical and Measured Data. *Sol. Energy* **1993**, *51*, 121–138. [CrossRef]
39. Gkikas, A.; Proestakis, E.; Amiridis, V.; Kazadzis, S.; Di Tomaso, E.; Marinou, E.; Hatzianastassiou, N.; Kok, J.F.; García-Pando, C.P. Quantification of the Dust Optical Depth across Spatiotemporal Scales with the MIDAS Global Dataset (2003–2017). *Atmos. Chem. Phys.* **2022**, *22*, 3553–3578. [CrossRef]
40. Papachristopoulou, K.; Fountoulakis, I.; Gkikas, A.; Kosmopoulos, P.G.; Nastos, P.T.; Hatzaki, M.; Kazadzis, S. 15-Year Analysis of Direct Effects of Total and Dust Aerosols in Solar Radiation/Energy over the Mediterranean Basin. *Remote Sens.* **2022**, *14*, 1535. [CrossRef]
41. Kosmopoulos, P.; Kazadzis, S.; El-Askary, H.; Taylor, M.; Gkikas, A.; Proestakis, E.; Kontoes, C.; El-Khayat, M. Earth-Observation-Based Estimation and Forecasting of Particulate Matter Impact on Solar Energy in Egypt. *Remote Sens.* **2018**, *10*, 1870. [CrossRef]

42. Fountoulakis, I.; Kosmopoulos, P.; Papachristopoulou, K.; Raptis, I.-P.; Mamouri, R.-E.; Nisantzi, A.; Gkikas, A.; Witthuhn, J.; Bley, S.; Moustaka, A.; et al. Effects of Aerosols and Clouds on the Levels of Surface Solar Radiation and Solar Energy in Cyprus. *Remote Sens.* **2021**, *13*, 2319. [[CrossRef](#)]
43. Dumka, U.C.; Kosmopoulos, P.G.; Ningombam, S.S.; Masoom, A. Impact of Aerosol and Cloud on the Solar Energy Potential over the Central Gangetic Himalayan Region. *Remote Sens.* **2021**, *13*, 3248. [[CrossRef](#)]
44. Dumka, U.C.; Kosmopoulos, P.G.; Patel, P.N.; Sheoran, R. Can Forest Fires Be an Important Factor in the Reduction in Solar Power Production in India? *Remote Sens.* **2022**, *14*, 549. [[CrossRef](#)]
45. International Renewable Energy Agency. Future of Solar PV. 2019. Available online: https://irena.org/-/media/Files/IRENA/Agency/Publication/2019/Nov/IRENA_Future_of_Solar_PV_2019.pdf (accessed on 18 June 2022).
46. National Renewable Energy Laboratory. Best Research-Cell Efficiency Chart. 2022. Available online: <https://www.nrel.gov/pv/cell-efficiency.html> (accessed on 18 June 2022).
47. Arias-Rosales, A.; LeDuc, P.R. Shadow modeling in urban environments for solar harvesting devices with freely defined positions and orientations. *Renew. Sustain. Energy Rev.* **2022**, *164*, 112522. [[CrossRef](#)]
48. Rao, A.; Pillai, R.; Mani, M.; Ramamurthy, P. Influence of dust deposition on photovoltaic panel performance. *Energy Procedia* **2014**, *54*, 690–700. [[CrossRef](#)]
49. PVGIS. Photovoltaic Geographical Information System. Available online: <http://re.jrc.ec.europa.eu/pvgis/> (accessed on 18 June 2022).
50. Bird, R.E.; Riordan, C. Simple Solar Spectral Model for Direct and Diffuse Irradiance on Horizontal and Tilted Planes at the Earth's Surface for Cloudless Atmospheres. *J. Appl. Meteorol. Climatol.* **1986**, *25*, 87–97. [[CrossRef](#)]
51. Wild, M. Global Dimming and Brightening: A Review. *J. Geophys. Res. Atmos.* **2009**, *114*, D00D16. [[CrossRef](#)]
52. Leibensperger, E.M.; Mickley, L.J.; Jacob, D.J.; Chen, W.-T.; Seinfeld, J.H.; Nenes, A.; Adams, P.J.; Streets, D.G.; Kumar, N.; Rind, D. Climatic Effects of 1950–2050 Changes in US Anthropogenic Aerosols—Part 1: Aerosol Trends and Radiative Forcing. *Atmos. Chem. Phys.* **2012**, *12*, 3333–3348. [[CrossRef](#)]
53. Inness, A.; Ades, M.; Agustí-Panareda, A.; Barré, J.; Benedictow, A.; Blechschmidt, A.-M.; Dominguez, J.J.; Engelen, R.; Eskes, H.; Flemming, J.; et al. The CAMS Reanalysis of Atmospheric Composition. *Atmos. Chem. Phys.* **2019**, *19*, 3515–3556. [[CrossRef](#)]
54. Gueymard, C.A.; Yang, D. Worldwide Validation of CAMS and MERRA-2 Reanalysis Aerosol Optical Depth Products Using 15 Years of AERONET Observations. *Atmos. Environ.* **2020**, *225*, 117216. [[CrossRef](#)]
55. Mortier, A.; Gliß, J.; Schulz, M.; Aas, W.; Andrews, E.; Bian, H.; Chin, M.; Ginoux, P.; Hand, J.; Holben, B.; et al. Evaluation of Climate Model Aerosol Trends with Ground-Based Observations over the Last 2 Decades—An AeroCom and CMIP6 Analysis. *Atmos. Chem. Phys.* **2020**, *20*, 13355–13378. [[CrossRef](#)]